NUMERICAL SIMULATION STUDY OF SILICA AND CALCITE DISSOLUTION AROUND A GEOTHERMAL WELL BY INJECTING HIGH pH SOLUTIONS WITH CHELATING AGENT

Tianfu Xu[1], Peter Rose[2], Scott Fayer[2], and Karsten Pruess[1]

[1]Earth Sciences Division, Lawrence Berkeley National Laboratory, 1 Cyclotron Road, Berkeley, CA 94720
e-mail: Tianfu_Xu@lbl.gov

[2]Energy and Geoscience Institute at the University of Utah • 423 Wakara Way suite 300 Salt Lake City, UT 84108

ABSTRACT

Dissolution of silica, silicate, and calcite minerals in the presence of a chelating agent (NTA) at a high pH has been successfully performed in the laboratory using a high-temperature flow reactor. The mineral dissolution and porosity enhancement in the laboratory experiment has been reproduced by reactive transport simulation using TOUGHREACT. The chemical stimulation method has been applied by numerical modeling to a field geothermal injection well system, to investigate its effectiveness. Parameters from the quartz monzodiorite unit at the Enhanced Geothermal System (EGS) site at Desert Peak (Nevada) were used. Results indicate that the injection of a high pH chelating solution results in dissolution of both calcite and plagioclase minerals, and avoids precipitation of calcite at high temperature conditions. Consequently reservoir porosity and permeability can be enhanced especially near the injection well.

CALCITE DISSOLUTION USING CHELATING AGENTS

Removal of calcite scaling from wellbores is commonly accomplished by injecting strong mineral acid (such as HCl). Injected strong acid tends to enter the formation via the first fluid entry zone, dissolving first-contacted minerals aggressively while leaving much of the rest of the wellbore untreated.

An alternative to the mineral acid treatment is the use of chelating agents such as ethylenediaminetetraacetic acid (EDTA) or nitrilotriacetic acid (NTA). Mella et al. (2006) performed lab experiments using EDTA and NTA to investigate the effectiveness of chelating agents for calcite dissolution in the formation. A laboratory reactor was designed and fabricated for investigating calcite dissolution using these agents under controlled conditions that simulate a geothermal reservoir; the setup and results will be discussed in the next section. Preliminary experimental data indicated that both EDTA and NTA are effective dissolution agents and that dissolution capacity increases with temperature.

Such agents have the ability to chelate (or bind) metals such as calcium. Through the process of chelation, calcium ions would be solvated by the chelating agent, driving calcite dissolution. The kinetics of calcite dissolution using chelating agents is not as fast as that using strong mineral acids. The lower dissolution rate allows the chelating agent to take a more balanced path through the formation and more evenly dissolve calcite in all available fractures, rather than following the first fluid entry zone and leaving the rest relatively untouched.

In the calcite chelating process, one EDTA molecule will associate with two Ca^{2+} ions,

$$EDTA^{4-} + 2Ca^{2+} = Ca_2EDTA \quad (1)$$

allowing theoretically for the dissolution of two moles of calcite per one mole of EDTA. Two NTA molecules are required to dissolve three calcite molecules.

$$2NTA^{3-} + 3Ca^{2+} = Ca_3NTA_2 \quad (2)$$

NUMERICAL MODELING METHOD

General Features

The modeling of the lab experiment and field example was done with the non-isothermal reactive geochemical transport program TOUGHREACT, whose physical and chemical process capabilities and solution techniques have been discussed by Xu and Pruess (2001) and Xu et al. (2006). The program uses integral finite differences for space discretization (IFD; Narasimhan and Witherspoon, 1976). The IFD method provides for flexible discretization using irregular grids, which is well suited for simulation of flow, transport, and fluid-rock interaction in heterogeneous and fractured rock systems with varying petrology and complex model boundaries due to the presence of engineered structures. For regular grids, the IFD method is equivalent to the

conventional finite difference method. An implicit time-weighting scheme is used for modeling flow, transport, and kinetic geochemical reactions.

The program can be applied to one-, two-, or three-dimensional porous and fractured media with physical and chemical heterogeneity, and can accommodate any number of chemical species present in liquid, gas and solid phases. A broad range of subsurface thermal-physical-chemical processes are considered under various thermohydrological and geochemical conditions of pressure, temperature, water saturation, ionic strength, and pH and Eh. Temporal changes in porosity and permeability due to mineral dissolution and precipitation are considered in the model. Changes in porosity are calculated from changes in mineral volume fractions. Several porosity-permeability relationships are considered in the simulator, including the cubic Kozeny-Carman grain model and Verma-Pruess model (1988).

Reaction Kinetics

Kinetics of mineral dissolution and precipitation is very important for chemical stimulation of an EGS reservoir. A general kinetic rate law for mineral dissolution and precipitation is used in TOUGHREACT (Lasaga et al., 1994)

$$r_n = \pm k_n A_n \left| 1 - \left(\frac{Q_n}{K_n} \right)^{\theta} \right|^{\eta} \qquad (3)$$

where n denotes kinetic mineral index, positive values of r_n indicate dissolution, and negative values precipitation, k_n is the rate constant (moles per unit mineral surface area and unit time) which is temperature-dependent, A_n is the specific reactive surface area of the mineral, K_n is the equilibrium constant for the mineral-water reaction written for the destruction of one mole of mineral n, and Q_n is the reaction quotient. The parameters θ and η must be determined from experiments; usually, but not always, they are taken equal to one (like in the present work).

For many minerals, the kinetic rate constant k can be summed from three mechanisms (Lasaga et al., 1994; Palandri and Kharaka, 2004), or

$$k = k_{25}^{nu} \exp\left[\frac{-E_a^{nu}}{R} \left(\frac{1}{T} - \frac{1}{298.15} \right) \right] + k_{25}^{H} \exp\left[\frac{-E_a^{H}}{R} \left(\frac{1}{T} - \frac{1}{298.15} \right) \right] a_H^{n_H} + k_{25}^{OH} \exp\left[\frac{-E_a^{OH}}{R} \left(\frac{1}{T} - \frac{1}{298.15} \right) \right] a_{OH}^{n_{OH}} \qquad (4)$$

where superscripts or subscripts nu, H, and OH indicate neutral, acid and base mechanisms, respectively, E_a is the activation energy, k_{25} is the rate constant at 25°C, R is gas constant, T is absolute temperature, a is the activity of the species; and n is power term (constant). Notice that parameters θ and η (see Eq. 1) are assumed the same for each mechanism.

MODEL CALIBRATION

A laboratory investigation of calcite dissolution together with silica dissolution using high pH solution with NTA was performed by Rose et al (2008**,** unpublished data). The flow reactor used is shown in Figure 1. The reactor flow cell was 6 inches long with a 1-inch internal diameter. The top 3 inches (7.62 cm) were filled with calcite chunks (30 g limestone) and the bottom 3 inches with silicate glass beads (or silica or quartz for different experiments). Water was injected from the top of the reactor with a flow rate of 3.333×10^{-5} kg/s (2 ml/min). Experiments were conducted for a temperature range from 150 to 300°C. The injection water was prepared by adding Na-NTA reagent and NaOH to distilled water; the resulting injection water had a NTA^{3-} concentration of 0.1 mol/kgw (w denotes H_2O). A high value of pH (pH = 11.5) was used because the maximum value of pH decreases with temperature. (The highest pH possible at 150°C is 11.63, while at 300°C it is 11.3). Measured total amounts of silica and calcite dissolved (in percent) after each experiment are presented in Figures 2 and 3. Each data point represents one experiment at a constant temperature. Most experiments were performed for a duration of 6 hours. For experiments with less duration time, the amount of dissolution was multiplied by a factor. For example, for a 3-hour experiment, the dissolution amount was multiplied by a factor of 2.

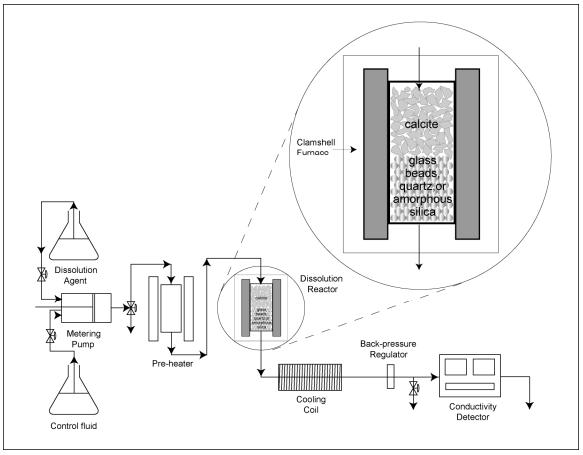

Figure 1: Schematic drawing of the high-temperature flow reactor

A 1-D model using TOUGHREACT was developed in order to simulate the dissolution experiment described above. Experimental data are then compared to model outputs and the model was calibrated as necessary to match the data. Such an approach will ultimately lead to improved forward-modeling of mineral dissolution in geothermal formations where operational parameters are more complex and varied.

Silica dissolution

For silica, the following expression is used in the calibration of its dissolution kinetic model:

$$r = Ak_{25}\exp\left[\frac{-E_a}{R}\left(\frac{1}{T}-\frac{1}{298.15}\right)\right]\left(1-\frac{c}{K}\right) \quad (5)$$

where r is silica dissolution rate (moles per unit mineral surface area and per unit time, mol/m^2/s), and c is the dissolved silica (SiO_2) concentration (mol/kgw). Other parameters are the same as defined in Eqs. (3) and (4). Eq. (5) has only one mechanism, which is a special case of the general multi-mechanism rate law defined in Eqs. (3) and (4).

To use rate expression (5), three parameters: A, k_{25}, and E_a are needed to be known. They can be obtained by calibrating measured data of silica dissolution. We used a reactive surface area of A = 98 cm^2/g, which is calculated by assuming a cubic array of truncated spheres (Sonnenthal, 2005). In fact, A and k_{25} are related by the product term in Eq. (5). Therefore, only k_{25} and E_a need to be calibrated for silica dissolution rate model. A large number of simulations corresponding to temperatures of 120, 140, 160, 200, 230, 250^{o}C were performed. The simulated total amounts of silica dissolved were matched to measurements by adjusting values of k_{25} and E_a (trial and error method).

Three curves (models) are presented together with measured data (Figure 2). Curve 1 has $K_{25} = 1.05\times10^{-8}$ mol/m^2/s and E_a = 39 kJ/mol, which fits well with measured silica dissolution data for temperature range from 160 to 250^{o}C. Curve 2 has $K_{25} = 1.85\times10^{-8}$ mol/m^2/s and E_a = 33.8 kJ/mol, which agrees with measured glass bead data for 160 to 220^{o}C temperatures. Curve 3 has $K_{25} = 1.14\times10^{-8}$ mol/m^2/s and E_a = 32.8 kJ/mol, which matches well with quartz dissolution data for 160-230^{o}C temperatures. Variation of the amount of silica dissolved with temperature is reflected by the activation energy term E_a.

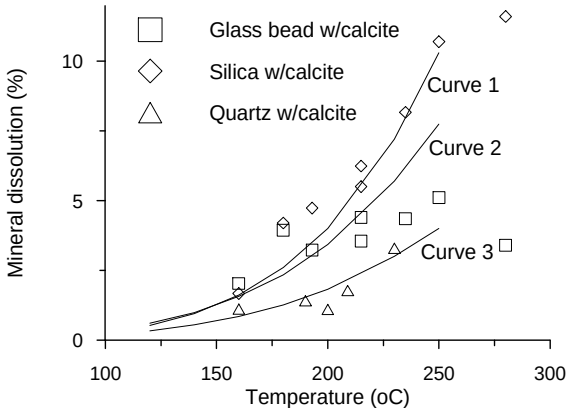

Figure 2: Measured total silica dissolution together with model results

Calcite dissolution

Calcite is assumed to react with aqueous species at local equilibrium. Calcite dissolution is driven by the chelating processes as described above. For the example of injection solution with NTA, the following reaction occurs, $2NTA^{3-} + 3Ca^{2+} = Ca_3NTA_2$. This chelating reaction is to proceed according to a kinetic rate. A simple linear kinetic rate expression for formation of Ca_3NTA_2 was used:

$$r_{Ca} = k_{Ca}C_{NTA} \quad (6)$$

where r_{Ca} is the rate (mol/kg$_W$/s), k_{Ca} is the rate constant (1/s), C_{NTA} is NTA concentration (mol/kg$_W$). As with the silica dissolution kinetic rate, we used an activation energy term to describe the temperature-dependence of k_{Ca}

$$k_{Ca} = k_{25}^{Ca}\exp\left[\frac{-E_a^{Ca}}{R}\left(\frac{1}{T}-\frac{1}{298.15}\right)\right] \quad (7)$$

Two parameters: k_{25}^{Ca} and E_a^{Ca} are needed to calibrate the chelating process model (or calcite dissolution model). The simulated total amounts of calcite dissolved were matched to measurements by adjusting values of the two parameters. The fitted curve in Figure 3 has k_{25}^{Ca} = 1.78×10^{-4} 1/s and E_a^{Ca} = 10 kJ/mol.

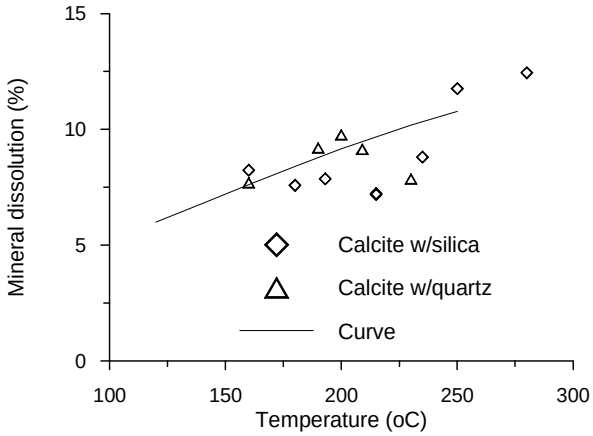

Figure 3: Measured total calcite dissolution together with model results.

NTA^{3-} complexing with Ca^{2+} results in a decrease in its concentration (Figure 4) and an increase in NTA_2CA_3 concentration along the column. Ca^{2+} concentration (Figure 5) remains low, maintaining calcite dissolution. Consequently dissolved carbon concentration increases continuously.

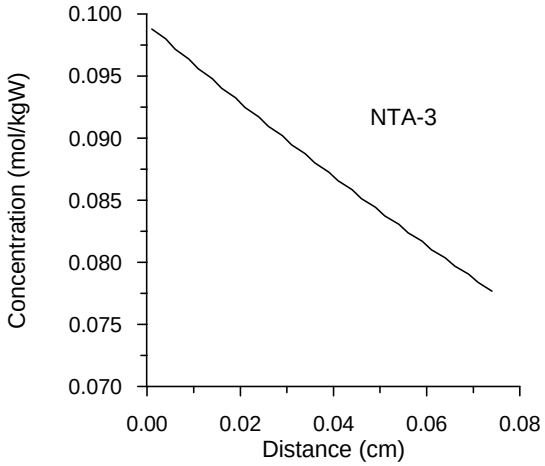

Figure 4: Simulated steady-state NTA^{3-} concentrations along the column for the calibrated calcite dissolution model.

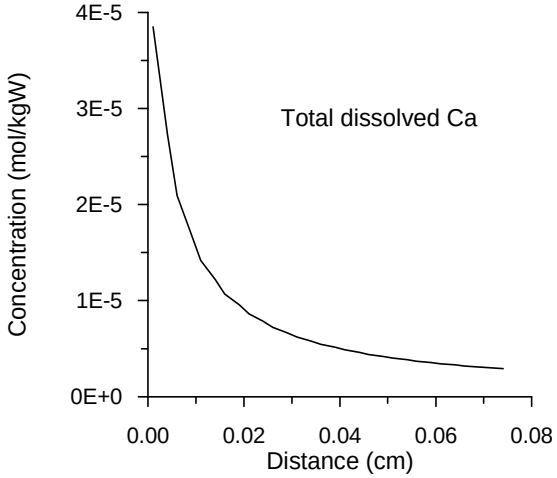

Figure 5: Simulated steady-state Ca^{2+} concentrations along the column for the calibrated calcite dissolution model.

FIELD APPLICATION

To investigate the effectiveness of injecting a high pH solution with chelating agent for the dissolution of calcite and silica minerals, we applied the chemical stimulation model to a geothermal injection well system using a mineralogical composition from the Desert Peak (Nevada) geothermal field. An industry-government cost-shared project at Desert Peak is underway to evaluate the technical feasibility of developing an Enhanced Geothermal System. The project is supported by US DOE, sponsored by Ormat Nevada, Inc., and technically coordinated by GeothermEx, Inc.

Model Setup

Geologic Setting and Mineralogy

In our model, the mineralogy was defined based on pre-tertiary unit 2 (pT2) in well DP 23-1, which is a quartz monzodiorite with 7-10 wt % quartz, 40-45 wt% plagioclase, 10-15 wt % potassium feldspar and 1-4 wt % sphene (Benoit et al., 1982; Lutz et al., 2004). A clinopyroxene and hornblende-bearing diorite directly overlies the main granodiorite intrusive body. The diorite is medium crystalline and contains primary hornblende phenocrysts with cores of clinopyroxene. The diorite is strongly propylitically altered to epidote, chlorite, pyrite and calcite, is moderately sericitized, and has also been thermally metamorphosed by the underlying granodiorite intrusive.

Initial mineralogical composition used in the modeling is summarized in Table 1. The compositions specified were based on the original crystalline rock mineralogy considering altered

fracture vein mineralogy. Plagioclase was modeled using 50% low-albite and 50% anorthite. Other minerals including epidote, pyrite, and biotite were not considered in the model, because their reactions with injection solution are slow and not important for the chemical stimulation purpose.

Table 1. *Initial mineralogical compositions used in the numerical modeling.*

Mineral	Quartz monzodiorite (% in terms of solid).
Quartz	9
Calcite	12
Low-albite	21.5
Anorthite	21.5
K-Feldspar	13
Chlorite	8
Illite	7
Others	8

Reaction kinetics

Table 2 lists parameters for the kinetics of mineral reactions used in the model. For quartz, specific reactive surface area and kinetic parameters k_{25} and E_a were taken from the calibration of the lab experiment (Curve 3 of Figure 3). Specific reactive surface areas for low-albite, anorthite, and K-feldspar are set the same as quartz. Surface area for chlorite and illite was from Sonnenthal et al. (2005), calculated assuming a cubic array of truncated spheres constituting the rock framework. The larger surface areas for these clay minerals are due to smaller grain sizes. Kinetic parameters k_{25} and E_a for low-albite, anorthite, K-feldspar kaolinite, chlorite, and illite were taken from Palandri and Kharaka (2004), who compiled and fitted experimental data reported by many investigators. The detailed list of the original data sources is given in Palandri and Kharaka (2004). Calcite dissolution is controlled by the kinetics of the chelating process and the calibrated parameters mentioned above were used.

Table 2. *Parameters for calculating kinetic rate constants of minerals. Note that A is specific surface area, k^{25} is kinetic constant at 25°C, E is activation energy, and n is the power term (Eq. 4).*

Mineral	*A* (cm^2/g)	*Parameters for kinetic rate law*							
		Neutral mechanism		*Acid mechanism*			*Base mechanism*		
		k^{25} ($mol/m^2/s$)	*E (KJ /mol)*	k^{25}	*E*	$n(H^+)$	k^{25}	*E*	$n(H^+)$
Quartz	98	1.14×10^{-8}	32.8						
Low-albite	98	2.754×10^{-13}	69.8	6.918×10^{-11}	65	0.457	2.512×10^{-16}	71	-0.572
Anorthite	98	2.754×10^{-13}	69.8	6.918×10^{-11}	65	0.457	2.512×10^{-16}	71	-0.572
K-feldspar	98	3.890×10^{-13}	38	8.710×10^{-11}	51.7	0.5	6.310×10^{-22}	94.1	-0.823
Chlorite	1516	3.02×10^{-13}	88	7.762×10^{-12}	88	0.5			
Illite	1516	1.660×10^{-13}	35	1.047×10^{-11}	23.6	0.34	3.020×10^{-17}	58.9	-0.4

Flow conditions

A 120 m thick reservoir formation with an injection well was modeled. A simple one-dimensional radial flow model was used, consisting of 50 radial blocks with logarithmically increasing radii. The 50 blocks cover a distance of 1000 m from the wall of the drilled open hole. Only the fracture network is considered in the model, with the assumption that the fluid exchange with the surrounding low permeability matrix is insignificant for the short period of chemical stimulation. An initial fracture permeability of 5.2×10^{-12} m^2 was assumed. A fracture porosity of 1% (ratio of fracture volume to the total formation volume) was assumed. The 1% volume of wall rock was included in the fracture domain, to allow minerals on the fracture wall interacting chemically with injection water. Therefore, initial porosity of the modeled fracture domain is 0.5, and permeability is 2.6×10^{-12} m^2. The uncertainty on the permeability specification doesn't affect modeling results of reactive transport and porosity enhancement (as long pressure buildup at wellbore can be afforded) because a constant injection rate was specified in the present study.

Conductive heat exchange with rocks of low permeability above and below this zone is an important process when injection temperature differs from the reservoir temperature. The confining layers are modeled as semi-infinite half spaces, and heat exchange is treated with a semi-analytical technique due to Vinsome and Westerveld (1980). Initial reservoir temperature is 210°C. An initial hydrostatic pressure of 20 MPa was assumed for about 2000 m depth. Hydrogeologic specifications of the 1-D radial flow problem are given in Table 3.

An injection temperature of 160°C was used. Injection water chemistry was the same as in the modeling of lab experiment, which was prepared by adding NTA agent and NaOH solution to steam condensate, and had a NTA^{3-} concentration of 0.1 mol/kg_W, a Na^+ concentration of 1.5 mol/kg_W, and a pH of 11.5. The initial water chemistry is in equilibrium with the initial mineralogy at a reservoir temperature of 210°C. An injection rate of 10 kg/s was applied for a period of half day. Reactive transport simulations were performed for up to one day, including a no-flow period after the 12-hour injection.

Table 3. *Geometric and hydrogeologic specifications for 1-D radial flow problem.*

Reservoir properties:	
Permeability	2.6×10^{-12} m^2
Porosity	0.5
Rock grain density	2750 kg/m^3
Rock specific heat	1000 J/kg/^oC
Thermal conductivity	2.4 W/m/^oC
Initial and boundary conditions:	
Pressure	200 bar
Temperature	210 ^oC
Injection conditions:	
Temperature	160 ^oC
rate	10kg/s
duration	12 hours

Results and Discussion

Injection of the high pH solution with chelating agent (NTA) results in increases in porosity along the flow path close to the injection well. Overall enhancement of porosity at different times obtained from the simulation is presented in Figure 6. Increases in porosity are mainly caused by dissolution of calcite, low-albite and anorthite (Figures 7, 9, and 10). The porosity increases to about 60% from an initial value of 50% close to the injection point. The enhancement of porosity extends to a radial distance of about 5 m.

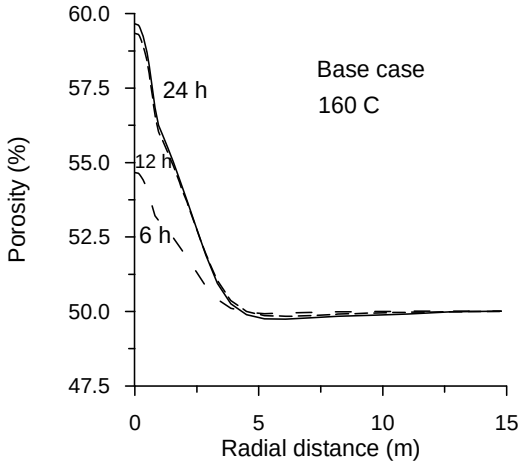

Figure 6. Distribution of porosity enhancements at different times obtained from the simulation (Initial porosity is 50%: half fracture space and half wall rock).

Calcite dissolves with maximum amount of 4.8% close to the injection point (Figure 7). A small amount of precipitation occurs at the moving front because increase in temperature causes decrease in calcite solubility. Amounts of quartz dissolution are very small because of low reaction rate (Figure 8). Generally low-albite dissolution occurs close to the injection point due to high pH, but later its precipitation occurs along the flow path because of lowered pH and high injected Na^+ concentration (Figure 9). Anorthite dissolves along the flow path because of low Ca^{2+} concentration (Figure 10). K-feldspar, chlorite, illite all dissolve close to the injection point and precipitate later along the flow path, but the amounts of their dissolution and precipitation are very small.

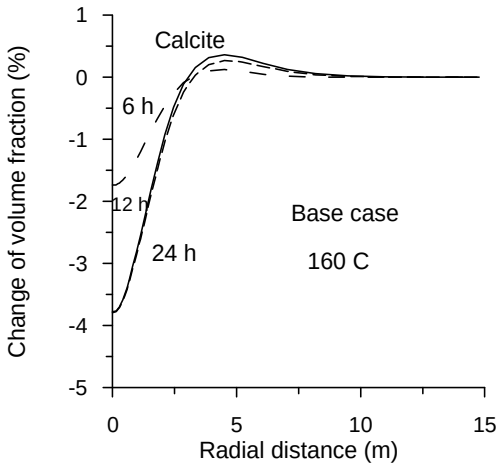

Figure 7. Changes of calcite abundance (in percentage of volume fraction, negative values indicate dissolution, positive precipitation) at different times.

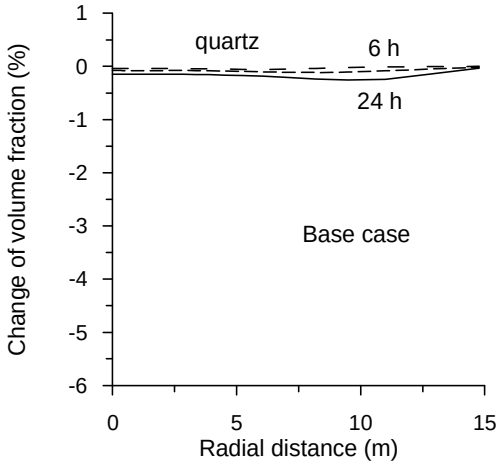

Figure 8. Changes of quartz abundance (in percentage of volume fraction) at different times.

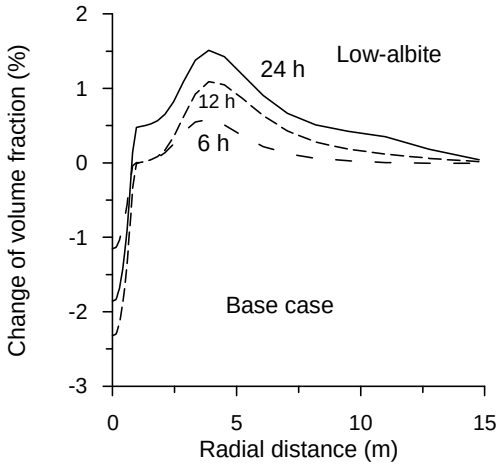

Figure 9. Changes of low-albite abundance (in percentage of volume fraction, negative values indicate dissolution, positive precipitation) at different times.

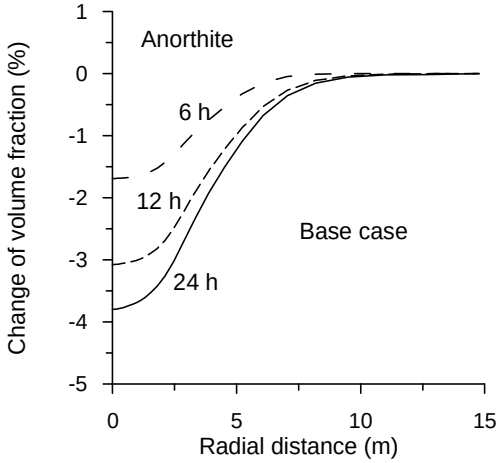

Figure 10. Dissolution of anorthite (in percentage of volume fraction) at different times.

NTA^{3-} concentration increases very slightly from 6 to 12 hours (Figure 11). After injection stops at 12 hours, NTA^{3-} is continuously complexing with Ca^{2+} and driving calcite dissolution. After 24 hours, NTA^{3-} is used up completely. Total dissolved carbon (mainly $CO3^{2-}$) concentrations increase gradually along the flow path because of calcite dissolution.

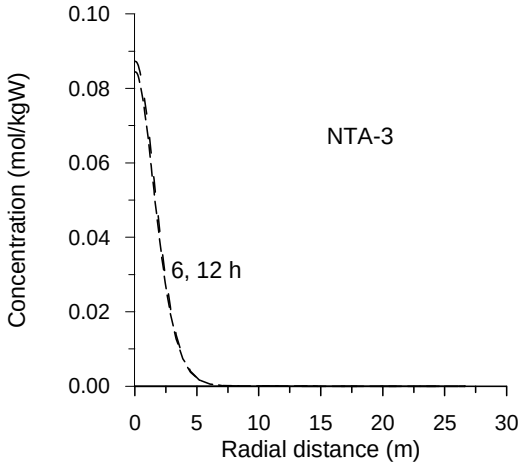

Figure 11. Distribution of NTA^{3-} concentrations at different times obtained from the simulation.

SUMMARY AND CONCLUSIONS

Dissolution of silica and calcite minerals in the presence of a chelating agent (NTA) at a high pH has been successfully performed in the laboratory using a high-temperature flow reactor. The mineral dissolution and porosity enhancement in the laboratory experiment has been reproduced by reactive transport modeling using TOUGHREACT, resulting in calibrated parameters for a dissolution model of calcite and silica minerals. The chemical stimulation method together with calibrated parameters has been applied by numerical modeling to a field geothermal injection well system. The crystalline rock unit of quartz monzodiorite from the site the Desert Peak EGS site was used. The injection of a high pH chelating (NTA) solution results in dissolution of both calcite and plagioclase minerals, and avoids precipitation of calcite at high temperature conditions. Consequently reservoir porosity and permeability can be enhanced in a region extending several meters around the injection well.

Many chemical and thermophysical factors affect mineral dissolution and associated enhancement in formation porosity and permeability, including mineral abundance and distribution in the formation, reaction kinetics, and injection rate. More detailed investigations will be conducted in the future when more data become available from field EGS demonstration projects.

ACKNOWLEDGEMENTS

The first and fourth authors (Tianfu Xu and Karsten Pruess) were supported by the Assistant Secretary for Energy Efficiency and Renewable Energy, Office of Geothermal Technologies, of the U.S. Department of Energy, under Contract No. DE-AC02-05CH11231. The second and third authors (Peter Rose and Scott Fayer) was supported by the same Agency under grant DE-FG36-04GO14295.

REFERENCES

Benoit, W.R., J.E. Hiner, and R.T Forest, 1982. Discovery and geology of the Desert Peak Geothermal Field: A case history, Nevada Bureau of Mines and Geology Bulletin 97, 82p.

Lasaga, A.C., Soler, J.M., Ganor, J., Burch, T.E., Nagy, K.L., 1994. Chemical weathering rate laws and global geochemical cycles. Geochimica et Cosmochimica Acta, 58, 2361-2386.

Lasaga, A.C., 1995. Fundamental approaches in describing mineral dissolution and precipitation rates. In: White, A.F., Brantley, S.L. (Eds.), Chemical Weathering Rates of Silicates Minerals, Reviews in Mineralogy, vol. 31. BookCrafters, Chelsea, MI, pp. 23–86.

Lutz, S.J., A.R. Tait, and C.L. Morris, 2004. Stratigraphic relationships in mesozoic basement rocks at the Desert Peak east EGS area, Nevada, In Proceedings of Twenty-Ninth Workshop on Geothermal Reservoir Engineering, Stanford University, Stanford, California.

Mella, M., Kovac, K., Xu, T., Rose, P., Mcculloch, J., Pruess, K., 2006. Calcite dissolution in geothermal reservoirs using chelants, In Proceedings of Geothermal Resources Council.

Palandri, J., Kharaka, Y.K., 2004. A compilation of rate parameters of water-mineral interaction kinetics for application to geochemical modeling. US Geol. Surv. Open File Report 2004-1068, 64 pp.

Rimstidt, J.D., Barnes H.L., 1980. The kinetics of silica-water reactions", *Geochim. Cosmochim. Acta*, 44, 1683-1699.

Rose, P., T. Xu, K. Kovac, M. Mella, and K. Pruess, 2007. Chemical stimulation in near-wellbore geothermal formations: silica dissolution in the presence of calcite at high temperature and high pH, In Proceedings of Thirty-Second Workshop on Geothermal Reservoir Engineering, Stanford University, Stanford, California, January 22-24, 2007.

Sonnenthal E., Ito, A., Spycher, N., Yui, M., Apps, J., Sugita, Y., Conrad, M., Kawakami, S., 2005, Approaches to modeling coupled thermal, hydrological, and chemical processes in the Drift Scale Heater Test at Yucca Mountain. *International Journal of Rock Mechanics and Mining Sciences*, 42, 6987-719.

Vinsome, P. K. W., and Westerveld, J., 1980. A simple method for predicting cap and base rock heat losses in thermal reservoir simulators. J. Canadian Pet. Tech., 19 (3), 87–90.

Verma, A. Pruess, K., 1988. Thermohydrological conditions and silica redistribution near high-level nuclear wastes emplaced in saturated geological formations: *Journal of Geophysical Research*, 93, 1159-1173.

Xu, T., and Pruess, K., 2001. Modeling multiphase non-isothermal fluid flow and reactive geochemical transport in variably saturated fractured rocks: 1. Methodology. Am. J. Sci., 301, 16-33.

Xu, T., Ontoy, Y. Molling, P., Spycher, N., Parini, M., Pruess, K., 2004. Reactive transport modeling of injection well scaling and acidizing at Tiwi Field, Philippines. *Geothermics*, v. 33(4), p. 477-491.

Xu, T., Sonnenthal, E.L., Spycher, N., Pruess, K., 2006. TOUGHREACT - A simulation program for non-isothermal multiphase reactive geochemical transport in variably saturated geologic media: Applications to geothermal injectivity and CO_2 geological sequestration, *Computer & Geoscience*, v. 32/2 p. 145-165.

Zerai , B., Saylor, B.Z., Matiso, G., 2006. Computer simulation of CO_2 trapped through mineral precipitation in the Rose Run Sandstone, Ohio. Applied Geochemistry, 21, 223-240.